

# Cluster model analysis of exotic decay in actinide nuclei

**EJ du Toit**

Department of Physics, University of Stellenbosch, Post Office Box 1529, Stellenbosch, 7599, South Africa

E-mail: [ejdutoit@sun.ac.za](mailto:ejdutoit@sun.ac.za)

**Abstract.** A simple method is described to determine the possible cluster structures forming within a nucleus. This is used to describe the multiple cluster decays seen from certain nuclei and reproduce exotic decay data for a range of actinide nuclei, using the Binary Cluster Model, along with a phenomenological potential. Further, energy spectra and  $B(E2)$  values are calculated in order to establish whether these cluster structures could exist within the nucleus as a bound state.

## 1. Introduction

The emission of a heavy ion was first observed experimentally by Rose and Jones [1], when they detected the emission of  $^{14}\text{C}$  from  $^{223}\text{Ra}$ . In the following years, decays via the emission of clusters heavier than Carbon and via the emission of multiple clusters were observed [2, 3, 4, 5], while several theoretical models were developed in order to understand this process of decay by reproducing experimental data and predicting other possible cluster decays [6, 7].

One of the more simple theoretical models is that of the Binary Cluster Model (BCM) [8], where a cluster consisting of  $(Z_2, N_2)$  protons and neutrons orbits an inert core of  $(Z_1, N_1)$  protons and neutrons as a description of the nucleus consisting of  $(Z_T, N_T)$  protons and neutrons, where  $Z_T = Z_1 + Z_2$  and  $N_T = N_1 + N_2$ . Exotic decay is then easily exhibited, by simply choosing the cluster as the emitted ion, and identifying the remaining nucleons as the core.

By utilizing the work of Gurvitz and Kalbermann [9, 10], the exotic decay half-life can be calculated with  $T_{1/2} = \frac{\hbar \ln 2}{\Gamma}$  where the decay width  $\Gamma$  is given by

$$\Gamma = \frac{\hbar^2 \exp \left[ -2 \int_{r_2}^{r_3} |p(r)| dr \right]}{2\mu \int_{r_1}^{r_2} \frac{1}{p(r)} dr} \quad (1)$$

with  $r_1$ ,  $r_2$  and  $r_3$  corresponding to the classical turning points; the intersection of  $Q$  and  $V(r)$ , where  $Q$  refers to the  $Q$ -value of the decay. The reduced mass is given by  $\mu = \frac{A_1 A_2}{A_1 + A_2}$ , and the classical momentum  $p(r) = \sqrt{\frac{2\mu}{\hbar^2}(Q - V(r))}$ .

Buck *et al.* successfully reproduced the exotic decay half-lives of several nuclei by using (1) [11, 12], along with a Woods-Saxon and cubic Woods-Saxon form of the nuclear potential [13], given by

$$V_N(r) = -V_0 \left( \frac{x}{1 + \exp[(r - R_0)/a]} + \frac{1 - x}{(1 + \exp[(r - R_0)/3a])^3} \right) \quad (2)$$

where the potential depth is given by  $V_0$ , the diffuseness by  $a$ , the radius by  $R_0$ , and the relative contributions made by the Woods-Saxon and cubic Woods-Saxon terms are indicated by  $x$ .

Experiments have shown, however, that it is possible for nuclei to decay via the emission of multiple clusters, which poses certain problems in describing such decays theoretically. Further, calculating the exotic decay half-life for nuclei for which no experimental decay data exists also poses a problem in selecting the core and cluster. To this end, a method has been developed which enables us to consider the nucleus as a mixture of up to four different core-cluster decompositions, each with an associated preformation probability [14, 15].

These core-cluster structures can account for multiple cluster emissions, and the decay half-lives can be computed, by weighting the decay width with the preformation probability, and comparing it to the experimental values, where applicable. Further confirmation of these cluster structures can be found by calculating energy spectra and  $B(E2)$  values within the BCM.

Section 2 provides a brief summary of the Binary Cluster Model, while Section 3 describes the method of determining the core and cluster sizes. Section 4 contains the results where this method has been applied on a range of nuclei.

## 2. Binary Cluster Model

The Binary Cluster Model (BCM) assumes that a cluster  $(A_2, Z_2)$  orbits an inert core  $(A_1, Z_1)$ . In order to satisfy the Pauli Exclusion Principle, the nucleons contained in the cluster have to be placed above the Fermi surface of the core nucleons. The global quantum number is introduced for this purpose, and defined as,

$$G = 2n + L = \sum_{i=1}^{n_c} (2n_i + l_i) \quad (3)$$

where  $n_c$  is the number of nucleons in the cluster. The values of  $n_i$  and  $l_i$  correspond to the filling of shell orbitals above the closed core, satisfying the Pauli principle by hand [8]. The quantum numbers  $L$  and  $n$  refer to the orbital angular momentum and the number of nodes contained in the wavefunction of the core-cluster relative motion, respectively.

For actinide nuclei, the value of  $G$  can be estimated through the simple scaling formula  $G = 5A_2$ , first introduced by Buck *et al.* [16]. This gives rise to a natural band of states, corresponding to the energies  $E_L$ , where  $L = 0, 2, 4, \dots$ , which can be calculated by using the Bohr-Sommerfeld (BS) relation [17],

$$\int_{r_1}^{r_2} \sqrt{\frac{2\mu}{\hbar^2} (E_L - V(r))} dr = (G - L + 1) \frac{\pi}{2} \quad (4)$$

where  $r_1$  and  $r_2$  represents the innermost classical turning points. The potential  $V(r)$  consists of three parts; a coulomb term  $V_c(r)$  [18]; a Langer-modified centrifugal potential

$V_L(r) = \frac{(L + \frac{1}{2})^2 \hbar^2}{2\mu r^2}$  [19]; and a nuclear potential given by the phenomenological Woods-Saxon and cubic Woods-Saxon form, given by (2). By fitting experimental decay data to the cluster emission of several thorium isotopes, the best-fit parameters were found to be,

$$a = 0.75 \quad x = 0.36 \quad V_0 = 54.7A_2 \quad G = 5A_2 \quad (5)$$

while the radius  $R_0$  is obtained by fitting its value to the energy of the ground state, such that (4) is satisfied. These parameters were used to investigate the cluster emission and -structure of nuclei known to undergo exotic decay.

### 3. Cluster Formation Probability

The advantage of the Binary Cluster Model (BCM) is that the emission of a heavy ion is very easily exhibited, although a consistent method of determining the core and cluster sizes are required. Experimental data serves as a good guide, but these data are mostly lacking. To this end, we investigate the hypothesis of utilizing the binding energy of core and cluster as a guide in determining these two components [14, 15].

From known exotic decay data, the most favourable combination seems to be if either the core or cluster is doubly, or at least singly, magic. The most tightly bound nuclei are then found by determining the partition of a fixed charge and mass  $(Z_T, A_T)$  into various possible pairs of nuclides with charge and mass values  $(Z_1, A_1)$  and  $(Z_2, A_2)$  which maximize the difference:

$$D(Z_1, A_1, Z_2, A_2) = [B_A(Z_1, A_1) - B_L(Z_1, A_1)] + [B_A(Z_2, A_2) - B_L(Z_2, A_2)] \quad (6)$$

between the actual binding energy  $B_A$  and some smoothly varying average  $B_L$  obtained from a liquid-drop mass formula.

Since even-even nuclei are more tightly bound than other nuclei, only even-even  $(Z_T, A_T)$ ,  $(Z_1, A_1)$  and  $(Z_2, A_2)$  are considered. The current version of the liquid-drop formula, or Semi-Empirical Mass Formula (SEMF), for even-even nuclei is used [20]

$$B_L = a_v A - a_s A^{2/3} - a_c \frac{Z(Z-1)}{A^{1/3}} - a_a \frac{(A-2Z)^2}{A} + \frac{a_p}{A^{1/2}} \quad (7)$$

where

$$a_v = 15.56 \text{ MeV} \quad a_s = 17.23 \text{ MeV} \quad a_c = 0.697 \text{ MeV} \quad a_a = 23.285 \text{ MeV} \quad a_p = 12 \text{ MeV} \quad (8)$$

The idea is to establish a consistent method where the only information required is the total charge and mass,  $(Z_T, A_T)$ , along with readily available mass tables and (6). Additional input stems from the experimental observation that electric dipole transitions in heavy nuclei are very weak, i.e.  $B(E1; 1^- \rightarrow 0^+) \approx 0$ . Within the BCM, this requires, to a good approximation [15]

$$\frac{Z_1}{A_1} = \frac{Z_2}{A_2} = \frac{Z_T}{A_T} \quad ; \quad \frac{N_1}{A_1} = \frac{N_2}{A_2} = \frac{N_T}{A_T} \quad (9)$$

where  $N$  represents the number of neutrons.

In order to satisfy (9), the nucleus is considered to consist of a mixture of up to four core-cluster decompositions, with associated probabilities. The clusters are neighbouring isotopes and isotones, to ensure the satisfaction of these equations. This allows us to select an arbitrary cluster charge  $\bar{Z}_2$  as plotting parameter, compute the corresponding mean neutron number  $\bar{N}_2$  according to

$$\bar{N}_2 = \frac{N_T \bar{Z}_2}{Z_T} \quad (10)$$

and determine the number of protons and neutrons contained in the cluster in such a manner that they bracket the mean values, i.e.

$$Z_2 \geq \bar{Z}_2 \geq Z_2 - 2 \quad ; \quad N_2 \geq \bar{N}_2 \geq N_2 - 2 \quad (11)$$

with weights

$$\begin{aligned} p(Z_2) &= (1/2)[\bar{Z}_2 - (Z_2 - 2)] \quad ; \quad p(Z_2 - 2) = (1/2)[Z_2 - \bar{Z}_2] \\ p(N_2) &= (1/2)[\bar{N}_2 - (N_2 - 2)] \quad ; \quad p(N_2 - 2) = (1/2)[N_2 - \bar{N}_2] \end{aligned} \quad (12)$$

while the weighted average  $\bar{D}(\bar{Z}_2, \bar{N}_2)$  is calculated as

$$\bar{D}(\bar{Z}_2, \bar{N}_2) = \sum_{Z_2, N_2} p(Z_2)p(N_2)D(Z_2, N_2). \quad (13)$$

This method allows us to select mean cluster charges across a range of values, and calculate the corresponding weighted average  $\bar{D}(\bar{Z}_2, \bar{N}_2)$ . These results can be plotted, with the maximum corresponding to the most likely mean cluster charge. Decomposing this mean cluster charge into four core-cluster decompositions will then reveal the most likely core-cluster structure of the parent nucleus, with its associated probability of formation.

#### 4. Results

In order to establish the possible core-cluster structures of a nucleus, it is necessary to determine the mean cluster charge  $\bar{Z}_2$  for which  $\bar{D}(\bar{Z}_2, \bar{N}_2)$  is a maximum. Figure (1) shows the plot of  $\bar{D}(\bar{Z}_2, \bar{N}_2)$  for  $^{226}\text{Th}$  as a function of cluster charge. Since the full calculation produces two peaks, corresponding to  $Z_2 = 7$  and  $Z_2 = 9$ , it is necessary to introduce some smoothing of the curve, in order to obtain a single maximum.

A previous method based on a Fourier-based filtering process has been used [14] to remove the irregularities, but a similar result can be obtained by simply averaging over neighbouring values. At a specific mean cluster charge  $\bar{Z}_2$ , an average value of  $\bar{D}(\bar{Z}_2, \bar{N}_2)$  is then obtained by averaging the value of  $\bar{D}(\bar{Z}_2, \bar{N}_2)$  from a set number of  $\bar{Z}_2$  values surrounding the mean cluster charge of interest.

This method eliminates irregularities, by producing a single maximum, and takes into account relative contributions from multiple peaks and regions next to peaks. For the example of  $^{226}\text{Th}$ , the two peaks corresponding to  $Z_2 = 7$  and  $Z_2 = 9$  is reduced to a single peak at  $Z_2 = 8$ , a cluster charge which is contained in both peaks of the full calculation, since only even-even clusters are considered, and should therefore be the most likely cluster charge.

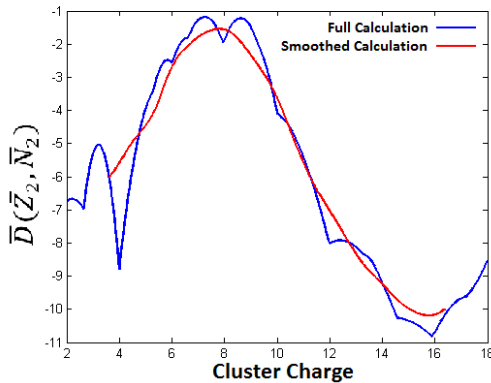


**Figure 1.** Calculations of  $\bar{D}(\bar{Z}_2, \bar{N}_2)$  as a function of cluster charge for  $^{226}\text{Th}$ .

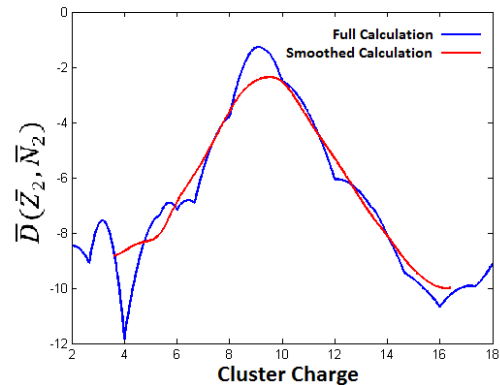


**Figure 2.** Calculations of  $\bar{D}(\bar{Z}_2, \bar{N}_2)$  as a function of cluster charge for  $^{230}\text{U}$ .

The maximum of  $\bar{D}(\bar{Z}_2, \bar{N}_2)$  for  $^{226}\text{Th}$  is obtained for a mean cluster charge of  $\bar{Z}_2 = 9.26$ , while for  $^{230}\text{U}$   $\bar{Z}_2 = 9.52$ . These mean cluster charges can be broken down into the four different core-cluster decompositions in order to reveal the possible cluster structures, along with their preformation probabilities. The exotic decay half-life can then be calculated for each cluster, and compared to experimental data, where available.

It was found that cluster decays which are not observed experimentally tend to have a small preformation probability and a long half-life, while the experimentally observed cluster decays tend to have greater preformation probabilities and shorter half-lives. Should the half-life for a

cluster decay be calculated to be orders of magnitude greater than another (observed) cluster decay, it will be nearly impossible to detect the decay of such a cluster, due to the competition from  $\alpha$ -decay and spontaneous fission that occurs on a much shorter time-scale.

A summary of the experimentally observed cluster decays seen in the actinide nuclei considered are shown in table 1. Of all the nuclei investigated, only one experimentally observed cluster was not predicted in the model: the  $^{28}\text{Mg}$  decay of  $^{238}\text{Pu}$ , although this shortcoming can be fixed by extending the model such that the nucleus consists of eight core-cluster structures. As can be seen from table 1, more than half of the calculated half-lives are in reasonable agreement with experimentally measured values.

The choice of parameters failed to reproduce the cluster decay of carbon and oxygen. While previous work shows [11, 12] that the BCM is not successful in accurately describing the cluster emission of oxygen, the inaccuracy in the carbon decay of  $^{224}\text{Ra}$  puts an additional bound on the mass and charge region of where the particular choice of parameters are valid. The potential parameters were chosen to reproduce the cluster decay of thorium isotopes, and applied to the calculations of radium, uranium and plutonium isotopes. A more consistent method of determining the potential parameters is therefore needed to accurately calculate exotic decay data for all nuclei considered, such as calculating parameter values from a microscopic potential, as was done for alpha clusters [21].

The calculated data show that multiple cluster decays can be described theoretically within this model, and that, where experiments are unable to determine the mass of an emitted cluster, this theoretical approach can be used to deduce the most likely emitted cluster. Such an example is the cluster emission of neon isotopes from  $^{232}\text{Th}$  and  $^{234}\text{U}$  [22].

**Table 1.** Summary of Exotic Decay Half-Lives of all experimentally observed decays. All considered actinide nuclei are shown with the emitted cluster and whether or not the model predicted this cluster. If the model predicts the cluster, the preformation probability  $P$  is also shown. Should the calculated half-life be within a factor 3 of the experimentally measured half-life, it is considered as a good approximation.

Nucleus	Cluster	P	Observed	Factor $\sim 3$	$T_{1/2}^{calc}[y]$	$T_{1/2}^{expt}[y]$
$^{222}\text{Ra}$	$^{14}\text{C}$	0.573	✓	✓	6590	$4017 \pm 528$
$^{224}\text{Ra}$	$^{14}\text{C}$	0.115	✓		$22.7 \times 10^8$	$(24.9 \pm 1.6) \times 10^7$
$^{226}\text{Th}$	$^{18}\text{O}$	0.099	✓		$21.9 \times 10^{10}$	$1.82 \times 10^9$
$^{228}\text{Th}$	$^{20}\text{O}$	0.38	✓		$24.0 \times 10^{13}$	$(16.9 \pm 1.4) \times 10^{12}$
$^{230}\text{Th}$	$^{24}\text{Ne}$	0.504	✓	✓	$13.3 \times 10^{16}$	$(13.0 \pm 0.52) \times 10^{16}$
$^{232}\text{Th}$	$^{24}\text{Ne}$	0.332	✓		$6.54 \times 10^{22}$	$5.06 \times 10^{21}$
$^{232}\text{Th}$	$^{26}\text{Ne}$	0.478	✓	✓	$4.87 \times 10^{21}$	$5.06 \times 10^{21}$
$^{230}\text{U}$	$^{24}\text{Ne}$	0.654	✓		$20.6 \times 10^{13}$	$(11.9 \pm 2.8) \times 10^{11}$
$^{232}\text{U}$	$^{24}\text{Ne}$	0.432	✓	✓	$13.7 \times 10^{12}$	$(77.4 \pm 4.5) \times 10^{11}$
$^{234}\text{U}$	$^{24}\text{Ne}$	0.025	✓		$48.7 \times 10^{18}$	$(27.3 \pm 6.7) \times 10^{17}$
$^{234}\text{U}$	$^{26}\text{Ne}$	0.815	✓	✓	$43.0 \times 10^{17}$	$(27.3 \pm 6.7) \times 10^{17}$
$^{234}\text{U}$	$^{28}\text{Mg}$	0.155	✓	✓	$15.8 \times 10^{17}$	$(17.5 \pm 4.3) \times 10^{17}$
$^{236}\text{Pu}$	$^{28}\text{Mg}$	0.129	✓	✓	$1.14 \times 10^{14}$	$1.43 \times 10^{14}$
$^{238}\text{Pu}$	$^{28}\text{Mg}$					$1.46 \times 10^{18}$
$^{238}\text{Pu}$	$^{30}\text{Mg}$	0.470	✓	✓	$2.51 \times 10^{18}$	$1.46 \times 10^{18}$
$^{238}\text{Pu}$	$^{32}\text{Si}$	0.070	✓		$4.46 \times 10^{18}$	$6.27 \times 10^{17}$
$^{240}\text{Pu}$	$^{34}\text{Si}$	0.454	✓	✓	$14.1 \times 10^{18}$	$(50.5 \pm 5.4) \times 10^{17}$

In order to determine whether the proposed cluster structures could exist within the nucleus as a bound state, structure observables such as energy spectra and  $B(E2)$  values were computed. The  $B(E2)$  values can be computed according to [23, 24]

$$B(E\ell; L_i \rightarrow L_f) = \frac{2\ell + 1}{4\pi} \left[ Z_1 \left( -\frac{A_2}{A} \right)^\ell + Z_2 \left( \frac{A_1}{A} \right)^\ell \right]^2 |\langle L_i 0 \ell 0 | L_f 0 \rangle|^2 |\langle \psi_{L_f} | r^\ell | \psi_{L_i} \rangle|^2 \quad (14)$$

where  $\psi_L$  is the wavefunction, and a small effective charge is introduced by replacing  $Z_i \rightarrow Z_i + \epsilon A_i$ , with  $\epsilon = 0.17$ .

Since the nucleus is considered to be a mixture of four core-cluster decompositions, the observables are calculated for each core-cluster decomposition, and a weighted average is calculated, according to the preformation probabilities. This weighted average value is then compared to the experimental value.

A summary of the calculated  $B(E2; 2^+ \rightarrow 0^+)$  and the highest known energy state are shown in table 2. Since the radius  $R_0$  is fitted to the  $Q$ -value of the ground state, the ground state energy is inherently correct, and should the highest known energy state correspond to the experimental value, all energy levels in between should be in good agreement with the experimental values.

From table 2 it can be deduced that the proposed cluster structures can exist as bound states, since all calculated  $B(E2)$  values, except for plutonium isotopes, are in agreement with the experimental values, as well as the energy levels. The inaccuracy in reproducing data of the plutonium isotopes places an additional bound on the region where the choice of parameters are valid.

**Table 2.** The calculated  $B(E2; 2^+ \rightarrow 0^+)$  values for all actinide nuclei considered are compared to known experimental values. The highest known energy levels are also calculated and compared to experimental values.

Nucleus	$B(E2)^{expt}$ [W.u.]	$B(E2)^{calc}$ [W.u.]	$E_L^*$	$E_L^{expt}$ [MeV $\pm$ eV]	$E_L^{calc}$ [MeV]
$^{222}\text{Ra}$	$111 \pm 9$	80	$E_{20}^*$	$3.29 \pm 11$	3.36
$^{224}\text{Ra}$	$97 \pm 4$	96	$E_{12}^*$	$1.41 \pm 4$	1.36
$^{226}\text{Th}$	$164 \pm 10$	145	$E_{20}^*$	$3.10 \pm 8$	2.84
$^{228}\text{Th}$	$167 \pm 6$	172	$E_{18}^*$	$2.41 \pm 7$	2.29
$^{230}\text{Th}$	$196 \pm 8$	206	$E_{24}^*$	3.82	2.59
$^{232}\text{Th}$	$198 \pm 11$	219	$E_{30}^*$	$5.16 \pm 3$	5.07
$^{230}\text{U}$	$222 \pm 27$	213	$E_{22}^*$	$3.24 \pm 4$	3.01
$^{232}\text{U}$	$241 \pm 21$	231	$E_{20}^*$	$2.66 \pm 9$	2.51
$^{234}\text{U}$	$236 \pm 10$	251	$E_{30}^*$	4.81	4.95
$^{236}\text{Pu}$	-	314	$E_{16}^*$	$1.79 \pm 5$	1.51
$^{238}\text{Pu}$	$285 \pm 5$	347	$E_{26}^*$	$4.27 \pm 9$	3.44
$^{240}\text{Pu}$	$287 \pm 11$	393	$E_{32}^*$	$5.82 \pm 8$	4.76

In conclusion, the proposed method of determining possible core-cluster decompositions within actinide nuclei and using the binary cluster model to calculate decay half-lives, electromagnetic transition probabilities and energy spectra, has shown that multiple cluster decays can be described theoretically, and that these core-cluster structures can possibly exist within heavy nuclei as bound states.

A fixed choice of potential parameters places a bound on the region where it can be applied, but within this region, the calculated decay values are in good agreement with experimental values. As such, it is possible to deduce the mass of emitted clusters where experiments are

unable to. Calculations of  $B(E2)$  values and energy spectra also indicate that these cluster structures can exist as bound states, although a more careful approach to obtaining the nuclear potential parameters might be needed.

## References

- [1] Rose H J and Jones G A 1984 *Nature* **307** p 245
- [2] Barwick S W, Price P B and Stevenson J D 1985 *Phys. Rev.* **C31** p 1984
- [3] Schicheng Wang, Price P B, Barwick S W, Moody K J and Hulet E K 1987 *Phys. Rev.* **C36** p 2717
- [4] Price P B 1989 *Annu. Rev. Nucl. Part. Sci.* **39** p 19
- [5] Tretyakova S P and Mikheev V L 1997 *Il Nuovo Cimento* **110A** p 1043
- [6] Greiner W 2007 *Rom. Rep. Phys.* **59** p 193
- [7] Bonetti R and Guglielmetti A 2007 *Rom. Rep. Phys.* **59** p 301
- [8] Buck B, Dover C B and Vary J P 1975 *Phys. Rev.* **C11** p 1803
- [9] Gurvitz S A and Kalbermann G 1987 *Phys. Rev. Lett.* **59** p 262
- [10] Gurvitz S A 1988 *Phys. Rev.* **A38** p 1747
- [11] Buck B, Merchant A C and Perez S M 1996 *Phys. Rev. Lett.* **76** p 380
- [12] Buck B, Merchant A C, Perez S M and Seals ME 2005 *J. Phys.* **G31** p 1499
- [13] Buck B, Merchant A C and Perez S M 1995 *Phys. Rev.* **C51** p 559
- [14] Buck B, Merchant A C, Horner M J and Perez S M 2000 *Phys. Rev.* **C61** p 024314
- [15] Buck B, Merchant A C and Perez S M 2000 *Few-Body Systems* **29** p 53
- [16] Buck B, Merchant A C, Perez S M and Tripe P 1994 *J. Phys.* **G20** p 351
- [17] Zettili N 2001 *Quantum Mechanics: Concepts and Applications* (John Wiley and Sons)
- [18] Buck B, Merchant A C and Perez S M 1992 *Phys. Rev.* **C45** p 2247
- [19] Langer R E 1937 *Phys. Rev.* **51** p 669
- [20] Martin B.R 2006 *Nuclear and Particle Physics: An Introduction* (John Wiley and Sons)
- [21] Ibrahim T T, Perez S M and Wyngaardt S M 2010 *Phys. Rev.* **C82** p 034302
- [22] du Toit E J, Wyngaardt S M and Perez S M 2015 *J. Phys. G* **42** p 015103
- [23] Wong S M 1990 *introductory Nuclear Physics* (Prentice Hall)
- [24] Ibrahim T T 2009 Ph.D. Thesis, Stellenbosch University (unpublished)